

# Length scales in orientational order of vertically aligned single walled carbon nanotubes

Christian Kramberger<sup>\*1</sup>, Theerapol Thurakitserree<sup>2</sup>, Hidetsugu Shiozawa<sup>1</sup>, Andreas Stangl<sup>1</sup>, Yudai Izumi<sup>3</sup>, Toyohiko Kinoshita<sup>3</sup>, Takayuki Muro<sup>3</sup>, Thomas Pichler<sup>1</sup>, and Shigeo Maruyama<sup>2</sup>

<sup>1</sup> Faculty of Physics, University of Vienna, Strudlhofgasse 4, 1090 Vienna, Italy

<sup>2</sup> Department of Mechanical Engineering, The University of Tokyo, 7-3-1 Hongo, Bunkyo-ku, Tokyo 113-8656, Japan

<sup>3</sup> Japan Synchrotron Radiation Research Institute, 1-1-1 Kouto, Sayo, Hyogo 679-5198, Japan

Received 18 April 2013, revised 2 September 2013, accepted 7 October 2013

Published online 6 November 2013

**Keywords** carbon nanotubes, orientational order, linear gas containers

\*Corresponding author: e-mail christian.kramberger-kaplan@univie.ac.at, Phone: +43 01 427772628, Fax: +43 01 427751375

We have studied the orientational order in films of vertically aligned single walled carbon nanotubes, by means of resonant Raman spectroscopy, resonant X-ray absorption, and direct imaging. These methods investigate the hierarchical morphology at different length scales. Here, we discuss the systematic

comparison of orientational order as function of wavelength in films with different inherent morphologies and provide thus a basis to quantitatively evaluate and compare the different experimental approaches.

© 2013 WILEY-VCH Verlag GmbH & Co. KGaA, Weinheim

**1 Introduction** Single walled carbon nanotubes (SWCNTs) are an exciting material. They offer a way to explore the beauty of one-dimensional physics empirically [1, 2]. Due to its principal versatility and scalability, the growth of SWCNTs by means of chemical vapor deposition (CVD) is an ever growing research area. The bulk properties and in particular the macroscopic anisotropy of SWNT specimen are defined by their internal morphology. The direct synthesis of vertically aligned single walled carbon nanotubes (VA-SWCNTs) provides bulk quantities of pure SWCNT. Different methods are available to quantify the orientational order in such samples. Optical absorption spectroscopy, Raman spectroscopy, and X-ray absorption have been utilized to derive actually very different results for VA-SWCNT [3–5]. The averaging over the probed volume as well as the employed wavelength are two crucial parameters that affect the apparent alignment, and have not been addressed specifically in the individual earlier reports. These factors may lead to utterly different findings when applying the textbook definition of orientational order to the different methods. Direct imaging as for instance in scanning electron microscopy has the added advantage, that there is also visual confirmation of an apparent orientational order, but the order parameter is not invariant under 2D projection.

Here, we revisit earlier specialized studies of the orientational order in differently vertically aligned single wall carbon nanotubes [6]. The alignment in such samples was studied either by second order Raman scattering or resonant X-ray scattering [5, 7, 8]. We apply an maximum amplitude wavelet image filter to extract and compare the orientational order directly from scanning electron micrographs. The key difference to earlier applied global Fourier analysis is the retained spatial resolution [9].

**2 Experimental** The synthesis of the different batches of vertically aligned SWCNTs is described elsewhere [6]. Very briefly, plain quartz substrates were dip-coated in Mo-acetylacetonate and Co-acetylacetonate solutions and backed in air at 400 °C. The catalyst particles were reduced under streaming Ar/3% H<sub>2</sub> until the furnace has reached 800 °C. After evacuation the substrate is exposed to static mixed vapor of ethanol and acetonitrile [10]. Zero and five percentage VA-SWCNT refer to the vol.% of acetonitrile in the liquid feedstock that was used for the synthesis of the two batches. The only further difference between the 0% and 5% batches are in the growth durations that were needed to yield comparable film thicknesses. While the growth of the 5% VA-SWCNT is saturated, the growth of 0% VA-SWCNT was

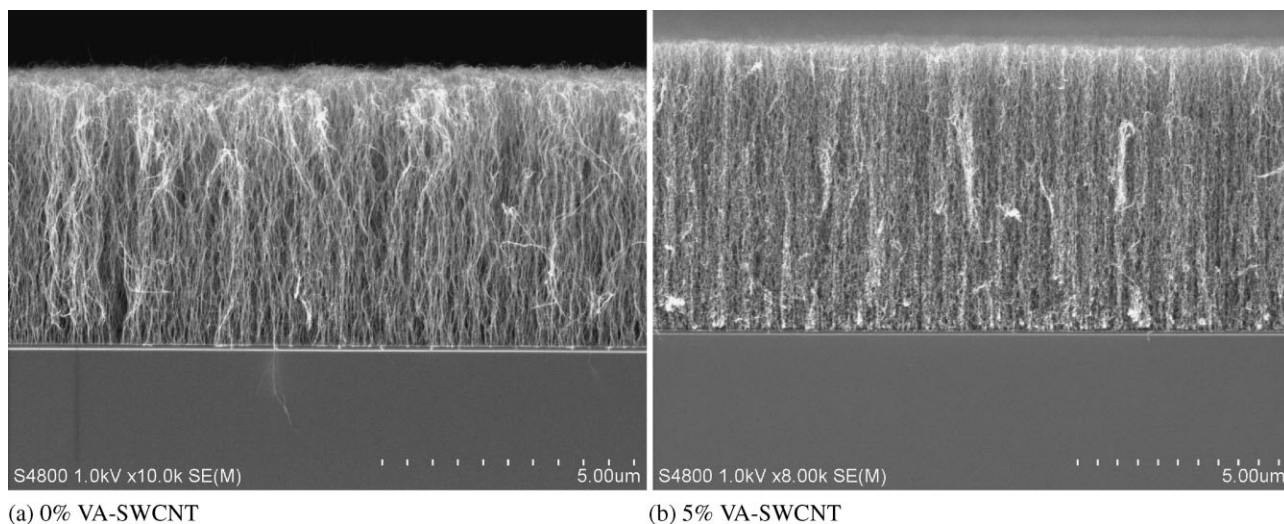


**Figure 1** Side view SEM micrograph of VA-SWCNT synthesized from pure ethanol feedstock (a) and 5% acetonitrile mixed feedstock (b).

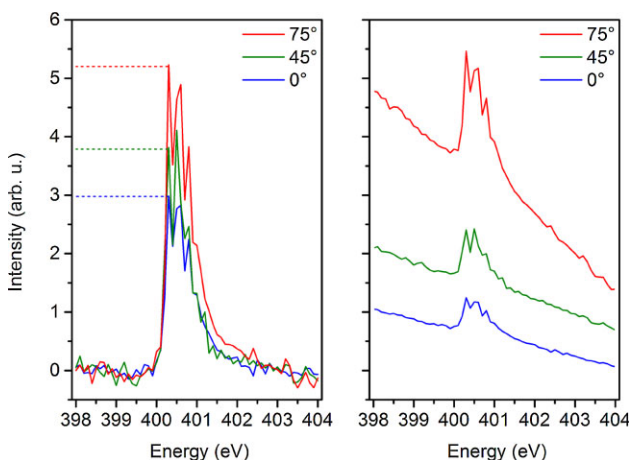
stopped after 2 min. Scanning electron microscopy (SEM) was performed at 1 kV acceleration voltage on a S-4800 microscope from Hitachi. X-ray absorption was measured at beamline BL27SU at the SPring-8 synchrotron facility. The vertical alignment of the encapsulated N<sub>2</sub> was investigated by varying the angle of incidence for p-polarized X-rays [5]. Polarization-dependent Raman spectra were obtained for 488 nm laser excitation and a 500 mm (Chromex 501is) spectrometer [8]. SEM images were processed by scanning for the highest amplitude of a finely tuned (1°) azimuth angle  $\Theta$  [11]. The sampling range, corresponding to the probing wavelengths, was set to be 100 nm. The lateral wavelet extension was kept at the resolution limit of 30 nm. For false color representation we used  $\cos^2(\Theta)$ .

**3 Discussion** The SEM micrographs in Fig. 1a and b are archetypical for the changes in mesoscopic morphology if ethanol feedstock and mixed feedstocks with acetonitrile are used. As viewed at a glance from the large distance there seems to be a better vertical alignment in Fig. 1b. However a closer inspection reveals that the individual constituents of the vertical columns are made up of more curls and kinks. In Fig. 1a, the overall morphology is not as straightly vertically aligned, but there seems to be much better alignment on a local scale. The visual inspection is by no means quantitative and will be corroborated by quantitative image processing to determine the order parameter  $\xi$ . In an uniaxial system, it is the coefficient of the first spherical harmonic in orientation distribution function and can be computed as  $\xi = \langle 3 \cos^2(\Theta) - 1 \rangle / 2$ .

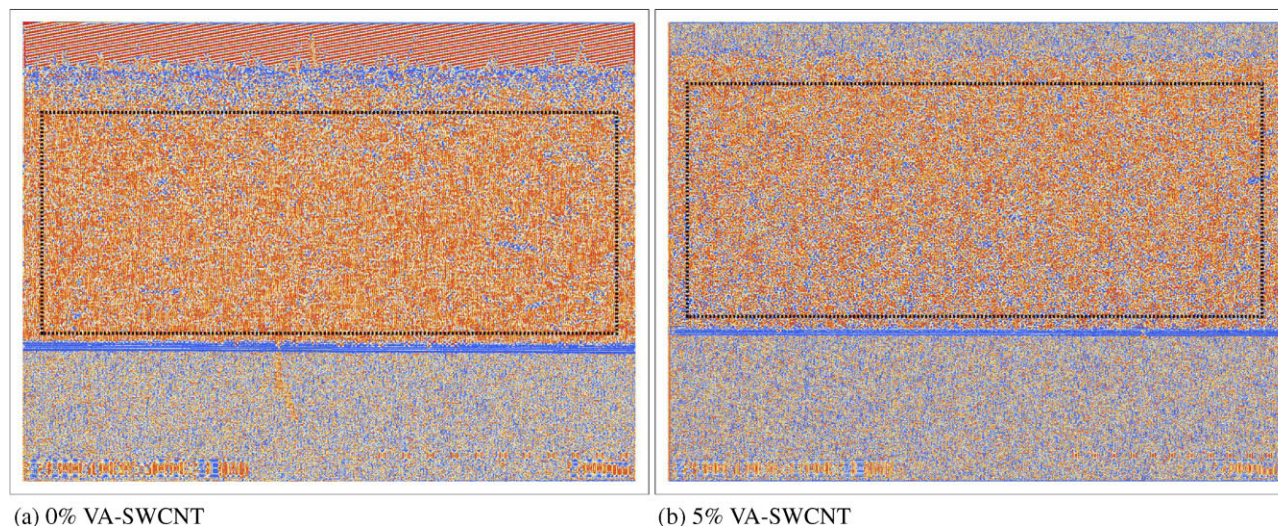
A side effect of the use of acetonitrile during synthesis is the encapsulation of N<sub>2</sub> molecules in the interior of VA-SWCNT. X-rays also allow to access the orientational order in the vertically aligned SWCNT [5]. The measure of order by comparison of the  $\pi$  and  $\sigma$  carbon orbitals is an atomistic local probe. The reported values  $\xi = 0.35$  for 0% VA-SWCNT and

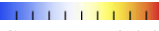
$\xi = 0.25$  for 5% VA-SWCNT confirm that the local order is on the atomic scale better in 0% VA-SWCNT.

While the evaluation of the orientational order parameter is straight forward for the intense C 1s absorption edge, the challengingly weak signal of the N 1s in (5%) VA-SWCNT can not be used directly to evaluate the intensities as a function of polarization [5]. The spectra in the right panel of Fig. 2 are *as measured* but offset by constant values to be plotted in the same range. As measured means that the drain current of the sample was divided by the drain current at the last focusing mirror. The actual values obtained by that common practice are as different as 0.09 and 0.35 for normal incidence and gracing angle incidence with 75°. The crucial notion here is that the slope of the background should not show any polarization dependence. The left panel of Fig. 2



**Figure 2** Nitrogen NEXAFS spectra for different angles of incidence with p-polarized X-rays. The right panel shows offset as measured intensities. The left panel compares the N 1s after correcting by slope of background.



**Figure 3** False color representation ( $[0, 1] \equiv$  ) of the local orientation  $\cos(\phi)^2$  in the SEM micrograph in Fig. 1 at a sampling range of  $\lambda = 100$  nm for 0% VA-SWCNT (a) and 5% VA-SWCNT (b). The highlighted areas were used to calculate the order parameter  $\xi$ .

shows the same spectra after they have been rescaled to the same slope before the slope was subtracted. In total, this treatment corresponds to a linear scaling, but it will not affect the depolarization ratio. By fitting an  $I(\Theta)A + B \cos^2(\Theta)$  dependence [12] to the data points the atomic orientational order  $\xi = (I(\pi/2) - I(0)) / (I(\pi/2) + 2I(0))$  is found to be 0.22, which follows closely the atomic alignment in the hosting (5%) VA-SWCNT.

The polarization dependence in side view Raman spectroscopy on 0% VA-SWCNT has been investigated recently [8]. The probed length scale is however in the range between 1 and  $2 \mu\text{m}$ . The evaluation of orientational order from Raman spectra is more elaborate. The incoming and outgoing dipole transitions combine to a  $\cos^4$  behavior, where depolarization ratio may not be used directly to access  $\xi$ . By modeling the entire orientation distribution function the optical order parameter  $\xi$  of the 0% VA-SWCNT is estimated to be better than 0.9. Since the spot size of probing laser is between 1 and  $2 \mu\text{m}$ , there may be no noticeable difference expected between 0% and 5% VA-SWCNT.

It is easy to see in the SEM micrographs why in the atomic range the order parameter as seen by X-rays, can be expected to be considerably lower than in the micrometer range as probed in microscopic Raman studies.

Conceptually, the SEM micrographs should contain the information about the orientational order as probed by different wavelengths. We show in Fig. 3a, a false color representation of the local wave vector direction. This is defined by the polar angle  $\phi$  of the most prominent amplitude within the sampling cut off of  $2\pi/\lambda$ . The colors are then mapped according to  $\cos(\Theta)^2$ . Red represents horizontal wave vectors and local vertical orientation, respectively. The VA-SWCNT films and their flat lying surface layer are easily recognizable in the filtered images. The contrast between the VA-SWCNT and the substrate cause a horizontal blue line

at the bottom. The overall red-tone of the SWCNT is visibly more intense in Fig. 3a, which suggest an indeed higher degree of alignment in 0% VA-SWCNT.

The projection into a SEM image causes an apparent  $\xi_{2D}$  as compared to the original  $\xi_{3D}$ . We evaluated  $\xi_{3D}$  and  $\xi_{2D}$  for a series of Maier–Saupe distribution functions [12]. The plot in Fig. 4 shows that  $\xi_{2D} > \xi_{3D}$ . The maximum overestimate found is  $\sim 0.15$ .

The local  $\cos(\Theta)^2$  is integrated for a selecting area of interest (dashed frames in Figs. 3a and b). At  $\lambda=100$  nm the order parameter  $\xi_{2D} = \langle 3 \cos^2(\Theta) - 1 \rangle / 2$  of the 0% VA-SWCNT is 0.59 and of the 5% VA-SWCNT is 0.48. The wavelength  $\lambda$  represents the length scale over that the SWCNT in the images may be locally linearized. We tested

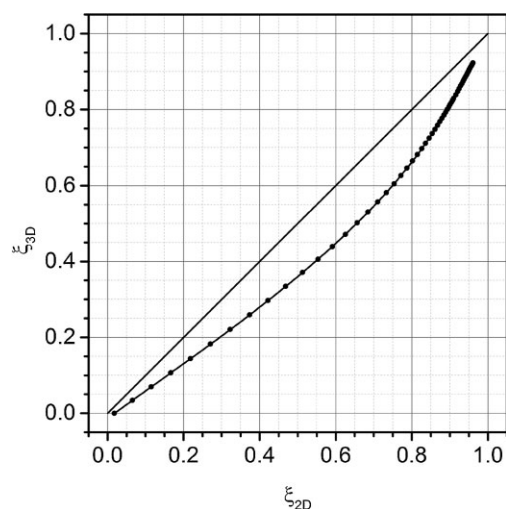


**Figure 4** Correlation between  $\xi_{3D}$  and  $\xi_{2D}$  if the long axis lies in the image. The dots are datapoints for Maier–Saupe [12] orientation distributions with  $0 \leq \alpha \leq 20$ .

the length scale dependence by increasing the  $\lambda$  to 300 nm. In this case  $\xi_{2D}$  increases to 0.74 and 0.64 for 0% and 5% VA-SWCNT, respectively.

The obtained order parameters  $\xi$  in two and three dimensions for the two different batches of vertically aligned SWCNT show at the investigated short and long wavelengths consistently the same trend. The differences can, in agreement to direct imaging, be ascribed to a more curled and kinked local morphology in the 5% VA-SWCNT. The mechanism responsible for vertical alignment is over-crowding. Indeed, different growth rates have been observed in multi-layered growth of 0% and 5% VA-SWCNT [13]. Different growth rates, as measured by optical density are related to different area densities of simultaneously growing SWCNT. Different area densities in turn are in agreement with more available space per nanotube and less strict alignment by less dense crowding [9].

The correlation between growth rate and orientational order is directly visible in Fig. 3b. There is an apparent vertical color gradient, which indicates better alignment in the top layer and lower alignment closer to the base of the film. Since the films grow from catalyst particles that reside at the root, the top part grew at an earlier time and faster rate than the bottom part [14]. The growth rate is decaying exponentially over time by statistical catalyst poisoning [15]. The lower initial growth rate, requires a saturated synthesis time for this thick 5% VA-SWCNT.

In direct comparison, the alignment visible as red tone in Fig. 3a does not show any noticeable gradient across the side wall. Indeed the 0% VA-SWCNT from Fig. 1a did grow much faster within 2 min before the growth was terminated early to match the thickness of the current 5% VA-SWCNT.

**4 Summary** We have employed a local wave vector image filter, to visualize the regional orientational order in VA-SWCNT. The orientational order parameters as probed by X-rays, direct imaging in SEM and Raman spectroscopy show always the same relative trend for differently dense VA-SWCNT. Additionally, a clear trend from low orientational order at the atomic scale, to intermediate alignment on the mesoscopic 100 nm length scale, to very high alignment on the micrometer scale reveals the hierarchical morphology of VA-SWCNT films.

**Acknowledgements** C.K. acknowledges the Austrian Academy of Sciences for the APART fellowship 11456. T.T. acknowledges support from the Higher Educational Strategic Scholarships for Frontier Research Network (CHE-PhD-SFR) granted by the Office of Higher Education Commission, Thailand. Beamtime at SPring-8 was granted for proposal 2012A1092.

## References

- [1] R. Saito, M. Dresselhaus, and G. Dresselhaus (eds.), *Physical Properties of Carbon Nanotubes* (World Scientific Publishing Company, London, 1998).
- [2] S. Reich, C. Thomsen, and J. Maultzsch, *Carbon Nanotubes: Basic Concepts and Physical Properties* (Wiley-VCH Verlag GmbH, Weinheim, Berlin, 2012).
- [3] Y. Murakami, E. Einarsson, T. Edamura, and S. Maruyama, *Phys. Rev. Lett.* **94**(8), 087402 (2005).
- [4] Y. Murakami, S. Chiashi, E. Einarsson, and S. Maruyama, *Phys. Rev. B* **71**(8), 085403 (2005).
- [5] C. Kramberger, T. Thurakitserree, H. Koh, Y. Izumi, T. Kinoshita, T. Muro, E. Einarsson, and S. Maruyama, *Carbon* **55**(0), 196–201 (2013).
- [6] T. Thurakitserree, C. Kramberger, P. Zhao, S. Aikawa, S. Harish, S. Chiashi, E. Einarsson, and S. Maruyama, *Carbon* **50**(7), 2635–2640 (2012).
- [7] H. H. Gommans, J. W. Alldredge, H. Tashiro, J. Park, J. Magnuson, and A. G. Rinzler, *J. Appl. Phys.* **88**(5), 2509–2514 (2000).
- [8] C. Kramberger, T. Thurakitserree, S. Chiashi, E. Einarsson, and S. Maruyama, *Appl. Phys. A* **109**(3), 509–513 (2012).
- [9] M. Xu, D. N. Futaba, M. Yumura, and K. Hata, *ACS Nano* **6**(7), 5837–5844 (2012).
- [10] H. Oshima, Y. Suzuki, T. Shimazu, and S. Maruyama, *Jpn. J. Appl. Phys.* **47**(4), 1982–1984 (2008).
- [11] H. Shiozawa, A. Bachmatiuk, A. Stangl, D. C. Cox, S. R. P. Silva, M. H. Rummeli, and T. Pichler, *Scientific Reports* **3**, 1840 (2013).
- [12] W. Maier and A. Saupe, *Z. Naturforsch. A* **14**(10), 882–889 (1959).
- [13] T. Thurakitserree, C. Kramberger, A. Kumamoto, S. Chiashi, E. Einarsson, and S. Maruyama, *ACS Nano* **7**(3), 2205–2211 (2013).
- [14] R. Xiang, Z. Y. Zhang, K. Ogura, J. Okawa, E. Einarsson, Y. Miyauchi, J. Shiomi, and S. Maruyama, *Jpn. J. Appl. Phys.* **47**(4), 1971–1974 (2008).
- [15] E. Einarsson, Y. Murakami, M. Kadowaki, and S. Maruyama, *Carbon* **46**(6), 923–930 (2008).